THE JOURNAL OF PHYSICAL CHEMISTRY C

ARTICLE

pubs.acs.org/JPCC

Decomposition and Reforming of Formic Acid on Supported Au Catalysts: Production of CO-Free H_2

A. Gazsi, T. Bánsági, and F. Solymosi*

Reaction Kinetics Research Group, Chemical Research Centre of the Hungarian Academy of Sciences, Department of Physical Chemistry and Materials Science, University of Szeged, P. O. Box 168, H-6701 Szeged, Hungary

ABSTRACT: The vapor-phase decomposition of formic acid was studied over Au supported on various materials, with the aim of producing CO-free H_2. With regards to the decomposition and H_2 formation, Au/SiO_2 was found to be the most active catalyst. The reaction started at 373 K and was complete at 523 K. Depending on the nature of the supports, significant differences were experienced in the reaction pathways. On Au deposited on SiO_2, CeO_2, and carbon Norit, dehydrogenation predominated, whereas on Al_2O_3, ZSM-5, and TiO_2-supported Au, dehydration of formic acid was favored. Pure CO-free H_2 was obtained on Au/SiO_2 and Au/CeO_2 at and below 473 K. No changes in activity or selectivity were observed within ~10 h. For most of the catalysts, the selectivity was improved by the addition of water to formic acid. In situ infrared spectroscopic studies revealed the formation of formate species even on Au/SiO_2, located exclusively on Au particles. The decomposition of HCOOH over Au/SiO_2 followed zero-order kinetics. The activation energy for the decomposition was 60.7 kJ mol^{-1}, and that for H_2 production was 58.5 kJ mol^{-1}.

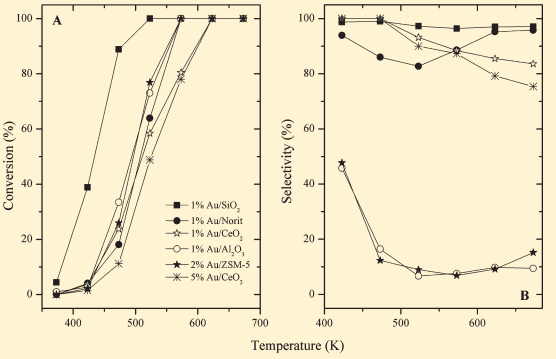

1. INTRODUCTION

The production of H_2, and particularly CO-free H_2, is a great challenge in heterogeneous catalysis. The decompositions of several carbon-containing compounds are used as sources of H_2. All have advantages and disadvantages. The decomposition of methanol gives virtually only H_2 and CO, with very low amounts of other compounds, but the complete elimination of CO cannot be achieved.[1] In contrast, in the decomposition of the readily available ethanol, the most frequently used raw material, several other compounds too are formed, and cleavage of the C−C bond necessitates the use of an active catalyst.[2] The production of H_2 from dimethyl ether demands first its hydrolysis into methanol to obtain a higher yield of H_2.[3] In the decomposition of hydrocarbons, the deposition of carbon results in early deactivation of the catalyst.[4−6] Supported Pt metals are frequently used as catalysts for the decomposition of the above compounds. However, in view of their high price, efforts are being made to replace them with cheaper, more active, stable catalysts. We have earlier reported that supported Mo_2C is a suitable material for activation of the above compounds.[7−9] Another new family of catalysts applied in this field comprise supported Au, which, in nanosize, has exhibited surprisingly high activities in several catalytic reactions.[10−12] Depending on the support, it effectively catalyzes the production of H_2 from methanol,[13] ethanol,[14] and dimethyl ether.[15]

It is somewhat surprising that the use of HCOOH, which is also a potential source of H_2 for fuel cells,[16,17] has received very little attention, though this reaction was widely used in the 1950s and 1960s to test the roles of the electronic properties of metals, alloys, and oxides in heterogeneous catalysis.[18−23] We recently reported that Mo_2C prepared by the reaction of MoO_3 with a multiwalled carbon nanotube and carbon Norit is an excellent and stable catalyst for the production of H_2 from formic acid virtually free of CO.[24] In their study of the decomposition of formic acid in the liquid phase, Zhou et al.[25] observed that the addition of Pd to Au/C and Ag/C resulted in very active and selective catalysts for the generation of H_2. Ojeda and Iglesia[26] have shown that isolated Au species on Al_2O_3 and TiO_2 can be used as an in situ source of H_2 from formic acid at high chemical potential. Ross et al.[27] discovered that Pd/C is a more active catalyst than Au/TiO_2 for the decomposition and reforming of formic acid, with selectivities of 95−99% at >400 K. In a recent comparative study, we found that Pt metals supported by carbon Norit are also effective catalysts in the vapor-phase decomposition of formic acid to generate H_2 with 95−99% selectivity.[28] H_2 completely free of CO was obtained in the reforming reaction of formic acid on Ir/Norit catalyst at 383−473 K. Promising results were also obtained in studies of the decomposition of formic acid on various metal complexes in solution.[29−31] In the present paper, we examine the catalytic performance of Au deposited on six different supports in the decomposition and reforming of HCOOH. The primary aim of this work is to identify the most active and selective Au catalysts and to establish experimental conditions under which H_2 can be produced in high yield and

Received: April 22, 2011
Revised: June 21, 2011
Published: July 05, 2011

virtually free of CO! In addition, the interaction of HCOOH with the catalyst samples is elaborated by FTIR spectroscopy, and kinetic measurements are carried out on the most active catalyst.

2. EXPERIMENTAL SECTION

Catalytic reactions were carried out at a pressure of 1 atm in a fixed-bed, continuous flow reactor consisting of a quartz tube (8 mm i.d.) connected to a capillary tube.[28] The flow rate was 40 mL/min. The carrier gas was Ar, which was bubbled through the formic acid at room temperature: its content was ~7.0%. In general, 0.3 g of the loosely compressed catalyst sample was used. The reaction products were analyzed with an HP 4890 gas chromatograph equipped with PORAPAK Q+S and a 30 m long HP-PLOT Al_2O_3 column. The conversion of formic acid was determined by taking into account the amount consumed. The selectivity of H_2 was calculated from the ratio of CO_2 concentration to the sum of CO_2 + CO. Multiplying this value with the conversion gave the H_2 yield. Fourier transformed infrared (FTIR) spectra of adsorbed formic acid were recorded with a BioRad FTS-155 spectrometer with a wavenumber accuracy of ± 4 cm^{-1}. In situ IR spectroscopic measurements were carried out in a diffuse reflectance infrared cell with CaF_2 windows, adapted to the FTIR spectrometer. X-ray photoelectron energy spectra (XPS) were taken with a Kratos XSAM 800 instrument using nonmonochromatic Al Kα radiation ($h\nu$ = 1486.6 eV) and a 180° hemispherical analyzer at a base pressure of 1×10^{-9} mbar. The sizes of the Au nanoparticles were determined by an electron microscope (Philips CM 20).

Supported Au catalysts with a gold loading of 1 or 5 wt % were prepared by a deposition−precipitation method. $HAuCl_4 \cdot aq$ (p.a., 49% Au, Fluka AG) was first dissolved in triply distilled water. After the pH of the aqueous $HAuCl_4$ solution had been adjusted to 7.5 by the addition of 1 M NaOH solution, a suspension was prepared with the finely powdered oxidic support, and the system was kept at 343 K for 1 h under continuous stirring. The suspension was then aged for 24 h at room temperature, washed repeatedly with distilled water, dried at 353 K, and calcined in air at 573 K for 4 h. The fragments of catalyst pellets were oxidized at 673 K and reduced at 673 K for 1 h in situ. The following compounds were used as supports: CeO_2 (Alfa Aesar, 50 m^2/g), Al_2O_3 (Degussa P 110 C1, 100 m^2/g), SiO_2 (CAB-O-SiL, 198 m^2/g), H-ZSM-5 with a SiO_2/Al_2O_3 ratio at 80 (Zeolit Intern. Süd-Chemie, 425 m^2/g), and activated carbon Norit (ALFA AESAR, 859 m^2/g). Carbon Norit was purified by treatment with HCl (10%) for 12 h at room temperature. Afterward, it was washed to have a Cl-free sample. After this treatment, the metal impurities, mainly Fe, determined by the ICP-AES method, amounted to less than 0.002%. HCOOH was the product of BDH, with a purity of 99.5%. Other gases were of commercial purity (Linde).

3. RESULTS

3.1. Characterization of Au Samples. The sizes of the Au nanoparticles were determined with an electron microscope and proved to be 1.9 nm for 1% Au/CeO_2, 6.5 nm for 1% Au/SiO_2, 5.7 nm for 1% Au/Norit, 5.5 nm for 1% Au/Al_2O_3, and 3.3 nm for 1% Au/ZSM-5. The XPS spectra of the supported Au catalysts used in the present work were taken previously.[14] The spectrum of the oxidized 1% Au/CeO_2 sample in the Au $4f_{7/2}$ region showed that most of the Au was in the Au^+ and Au^{3+} states. After reduction of the sample at 673 K, the intensity of the BE for Au^{3+} decreased and that of Au^0 developed. Concerning the XPS region of Ce in the oxidized catalyst, the dominant peaks at 882.6 and 898.4 eV were due to Ce^{4+}. The shoulders at 885.1 and 900.4 eV, however, revealed the presence of Ce^{3+} in the starting material. This indicated that the deposition of Au on CeO_2 leads to a partial reduction of the Ce^{4+} on the surface. These features were more evident after reduction of Au/CeO_2 at higher temperatures. Following the oxidation of 2% Au/SiO_2, the peaks in the Au 4f region demonstrated the presence of Au^{3+} and Au^+. Reduction at 673 K increased the intensity of the Au^0 peak, but, similarly as for 1% Au/CeO_2, did not eliminate Au^+ on the surface. On the oxidized Au/Norit sample, there were equal amounts of Au^{3+} and Au^+. After reduction, the BE peak for Au^0 also appeared.

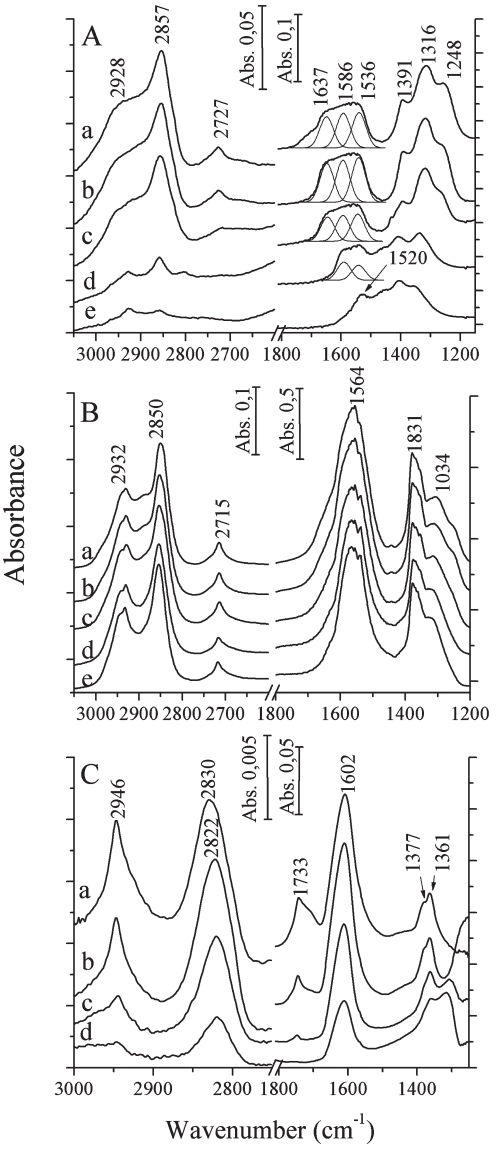

Figure 1. FTIR spectra of adsorbed HCOOH on 1% Au/CeO_2 (A), CeO_2 (B), and 1% Au/SiO_2 (C) at 300 K and after subsequent degassing at different temperatures: (a) 300, (b) 373, (c) 473, (d) 523, and (e) 573 K.

3.2. Infrared Spectroscopic Studies. Figure 1 depicts the IR spectra of HCOOH adsorbed on different samples (T_R = 673 K)

at 300 K and heated to different temperatures under continuous degassing. On 1% Au/CeO_2, absorption bands were observed at 2928, 2857, and 2727 cm^{-1} in the C−H stretching region. In the low-frequency range, a broad absorption feature between 1640 and 1500 cm^{-1} could be deconvoluted into peaks at 1637, 1586, and 1536 cm^{-1}. Well-detectable absorption bands also appeared at 1391, 1316, 1248, and 1081 cm^{-1}. At higher HCOOH exposure, a feature was seen at 1728 cm^{-1} (not shown). Heating of the sample caused the attenuation of all the bands and the disappearance of the band at 1728 cm^{-1} even at 373 K. Virtually identical spectra were measured following the adsorption of formic acid on pure CeO_2, with the difference that the bands were much more stable. The results obtained on 1% Au/SiO_2 deserve special attention. In the high-frequency region, nearly the same absorption bands were obtained as on the previous catalysts. We also detected a band at 1733 cm^{-1}, a very intense absorption at 1602 cm^{-1}, and less intense ones at 1377 and 1361 cm^{-1}. When the adsorbed layer was heated under continuous degassing, the 1733 cm^{-1} band disappeared at 523 K, but the spectral feature at 1602 cm^{-1} was detected even after evacuation at 573 K. When the Au content was increased to 5%, the intensities of the low-frequency bands at 1600, 1377, and 1361 cm^{-1} were somewhat stronger, but their thermal stabilities remained practically unaltered. IR measurements on the pure supports free of Au yielded very similar spectra, with the exception of SiO_2, where no absorption bands appeared in the range of 1700−1500 cm^{-1}. Table 1 lists the characteristic vibrations of HCOOH and formate species formed, together with their possible assignments.

Table 1. Vibrational Frequencies (in cm^{-1}) Observed Following the Dissociative Adsorption of HCOOH and Their Assignment

assignment	CeO_2	Au/CeO_2	Au/SiO_2
ν_a(OCO) and CH def.	2953		
ν(CH) formic acid	2928	2928	2946
ν(CH)	2871	2857	2830
ν_a(OCO) + δ_a(CH)	2737	2727	
ν(O)	1668	1637	
ν_a(OCO)	1555	1586	1602
ν_s(OCO)	1386	1391	1377
ν_s(OCO)	1369	1316	1361
CO	1288	1248	

3.3. TPD Measurements. TPD spectra for various products after the adsorption of formic acid on catalysts are displayed in Figure 2. The release of a very small amount of adsorbed formic acid from pure CeO_2 began above 300 K and proceeded continuously up to 450 K. The desorption of other compounds, CO and CO_2, started above 500 K, resulting in one maximum at ∼570 K. Much smaller amounts of H_2 were measured, at Tp = 600 K. Similar TPD spectra were obtained for 1% Au/CeO_2, with the differences that the evolution of H_2 was already observed above 400 K and the TPD peaks were wider. Divergent TPD curves were registered for Au/SiO_2 and Au/Norit (not shown), where, besides the weakly bonded HCOOH, only small amounts of CO_2 and H_2 desorbed between 350 and 500 K without CO.

3.4. Catalytic Studies. Figure 3A shows the conversion of formic acid on 1% Au supported on various materials. It appears that the catalytic performance of the Au catalyst is markedly influenced by the nature of the support. On the most active catalyst, Au/SiO_2, decomposition began at 373 K and total conversion was reached at 523 K. There was very little difference in efficiency between the other Au samples. Interestingly, further loading of the Au content on the CeO_2 to 5% caused a lower conversion at each temperature. On CeO_2-based catalysts, traces of methanol and formaldehyde were also detected.

The products of the reaction varied with the nature of the support. The selectivity for H_2 formation was 100% on Au/CeO_2 at 423−473 K, but was lower at higher temperature. The selectivity was also 100% on Au/SiO_2 at 373 K, which decreased to 98% at 423−473 K and 97% at 523 K, when total decomposition of the HCOOH occurred. High selectivities (95−84%) were also measured on Au/Norit. The lowest selectivity for H_2 (∼10%) was found on Au/Al_2O_3 and Au/ZSM-5. The

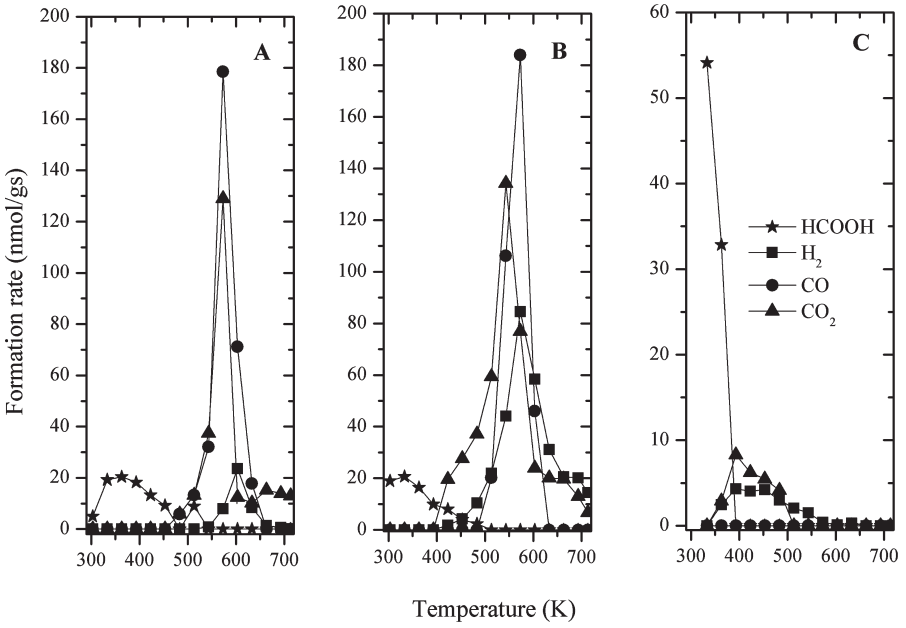

Figure 2. TPD spectra following the adsorption of HCOOH at 300 K on 1% Au/CeO_2 (A), CeO_2 (B), and 1% Au/SiO_2 (C).

dx.doi.org/10.1021/jp203751w |J. Phys. Chem. C 2011, 115, 15459–15466

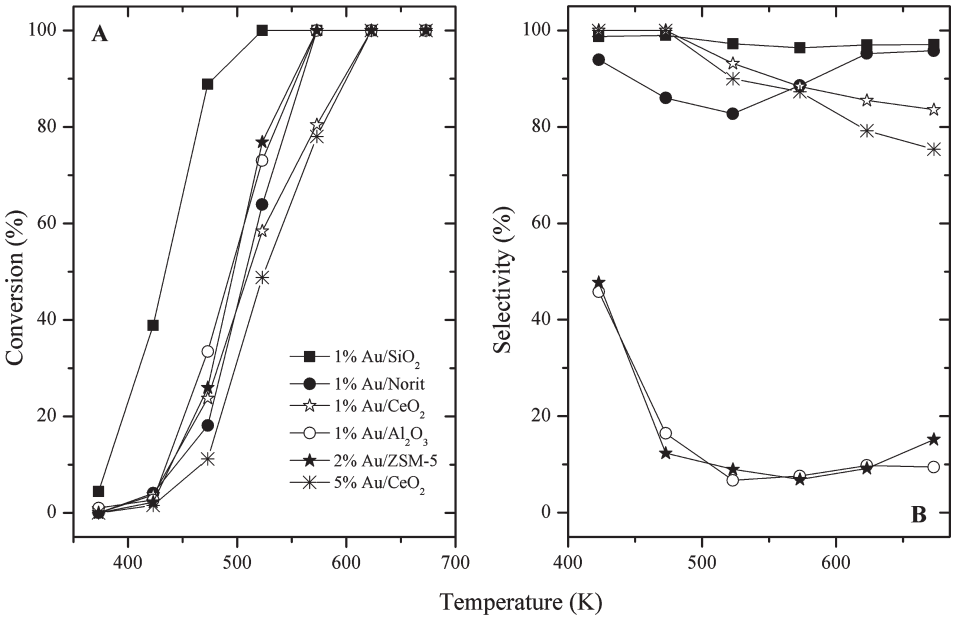

Figure 3. Conversion of formic acid (A) and the selectivity of H_2 formation (B) on supported Au catalysts as a function of temperature.

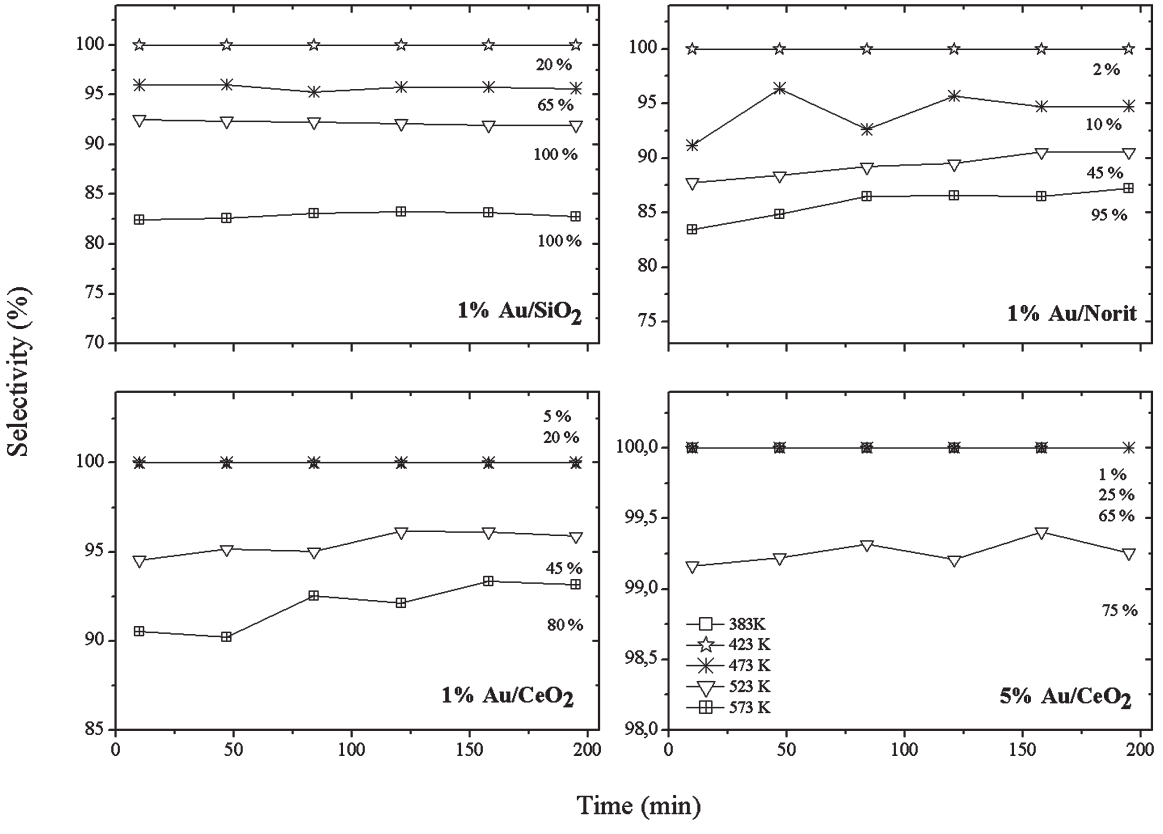

Figure 4. Selectivity of H_2 formation in the decomposition of HCOOH on various supported Au catalysts in time on stream at different temperatures. Conversion (in percent) of HCOOH is indicated.

selectivities for H_2 formation as a function of temperature are plotted in Figure 3B.

After determination of the effects of temperature, the reaction of formic acid was followed in time on stream at the total decomposition at 623−673 K. No or only a very slight decay was experienced in the conversion of HCOOH and in the selectivity of H_2 production in the measured time interval of ∼7 h. High stability was experienced at lower temperatures, when the selectivity for hydrogen was higher. CO-free H_2 was obtained on 1% Au/SiO_2 and on 1−5% Au/CeO_2 at 383−473

dx.doi.org/10.1021/jp203751w |J. Phys. Chem. C 2011, 115, 15459–15466

Table 2. Mean Particle Size Determined by TEM, Dispersion, and Turnover Frequencies for the Decomposition of HCOOH and for H_2 Production

catalysts	mean particle size, nm	dispersion	TOF_{H_2} and TOF_{HCOOH} at 473 K, s^{-1}	
1% Au/SiO_2	6.5	0.21	1.951	2.082
1% Au/Norit	5.7	0.25	0.297	0.317
1% Au/CeO_2	1.9	0.73	0.082	0.119
1% Au/Al_2O_3	5.5	0.25	0.005	0.439
1% Au/ZSM-5	3.3	0.43	0.027	0.222

K. Selectivity data measured at different temperatures are displayed in Figure 4. The influence of CO addition (about 10% of the HCOOH) on the Au/SiO_2 and Au/CeO_2 catalysts revealed practically no alteration in either the conversion or the selectivity for H_2.

Similar measurements were carried out with the oxidic supports treated in the same way as the Au-containing samples. In harmony with the previous studies,[20,21] the decomposition of formic acid, mainly the dehydration process, also occurred on the pure oxides. The conversion remained below 5−15% even at 523 K, which clearly indicates the significant catalytic effect of Au. Some important data for the decomposition of formic acid on various catalysts are presented in Table 2. Taking into account the dispersity of supported Au, the specific activities in terms of turnover frequencies (N_{H_2}, rates per surface Au atom) were calculated at 473 K. This gave the following activity sequence: Au/SiO_2, Au/Norit, Au/CeO_2, Au/ZSM-5, and Au/Al_2O_3.

To establish which adsorbed species exist on the surface under dynamic conditions, we performed FTIR spectroscopic studies in situ during the catalytic reaction in a flow of a gaseous mixture of HCOOH + Ar at 383−523 K. Spectra are presented in Figure 5. On 1% Au/CeO_2, besides the intense absorption band due to formic acid at 1720−1730 cm^{-1} (not shown), intense spectral features appeared at 1635, 1557, 1388, 1344, 1205, and 1125 cm^{-1} at 383 K. On elevation of the reaction temperature to 423−523 K, new absorption features developed at 1425 and 1409 cm^{-1}, the other absorption bands remaining unaltered (Figure 5A). When the stream of HCOOH + Ar was changed to pure Ar, we experienced only slight decreases in the intensities of these absorption bands. Similar results were obtained for pure CeO_2, when the vibration at 1565 cm^{-1} was much stronger (Figure 5B). A different picture was obtained for 1% Au/SiO_2, however. Besides the intense spectral feature due to molecular HCOOH at ~1750 cm^{-1}, weak absorption bands appeared at 1584, 1351, 1288, 1216, 1140, and 1085 cm^{-1} (Figure 5C).

On 1% Au/SiO_2, kinetic measurements were performed at low conversion, below ~10%. The partial pressure of formic acid was varied, keeping the total flow rate at 40 mL min^{-1} by adding Ar ballast to the system. The reaction of formic acid in the temperature range of 393−433 K under these conditions followed zero-order kinetics. The Arrhenius plots yielded 60.7 kJ mol^{-1} for the activation energy of the decomposition of formic acid and 58.5 kJ mol^{-1} for the formation of hydrogen.

3.5. Reforming of HCOOH. The effects of H_2O on the reaction of HCOOH depended sensitively on the nature of the support. The conversion was only slightly influenced on most of the catalysts. The reforming of formic acid was followed in time on stream at between 383 and 573 K. Data determined for various samples demonstrated that, apart from minor fluctuations, little change occurred (Figure 6). As the selectivity for H_2

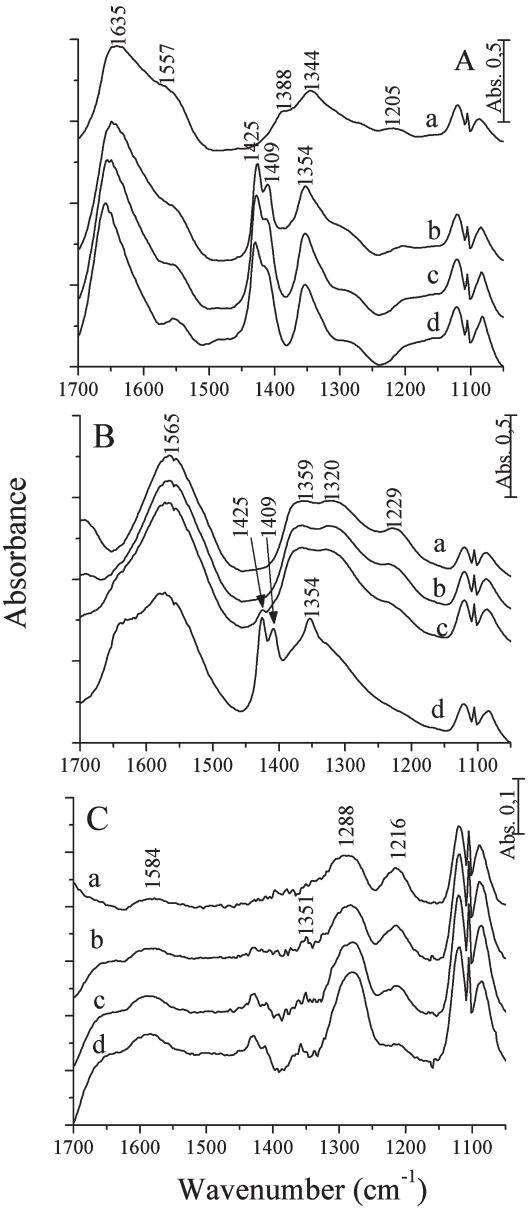

Figure 5. In situ IR spectra obtained during the decomposition of formic acid at different temperatures on 1% Au/CeO_2 (A), CeO_2 (B), and 1% Au/SiO_2 (C): (a) 383, (b) 423, (c) 473, and (d) 523 K.

was very high (even 100%) in the decomposition at lower temperatures, the positive effect of H_2O on this value appeared mostly at higher reaction temperatures. To judge the efficiency of the catalyst in the generation of H_2, we calculated the yield of H_2

dx.doi.org/10.1021/jp203751w |J. Phys. Chem. C 2011, 115, 15459–15466

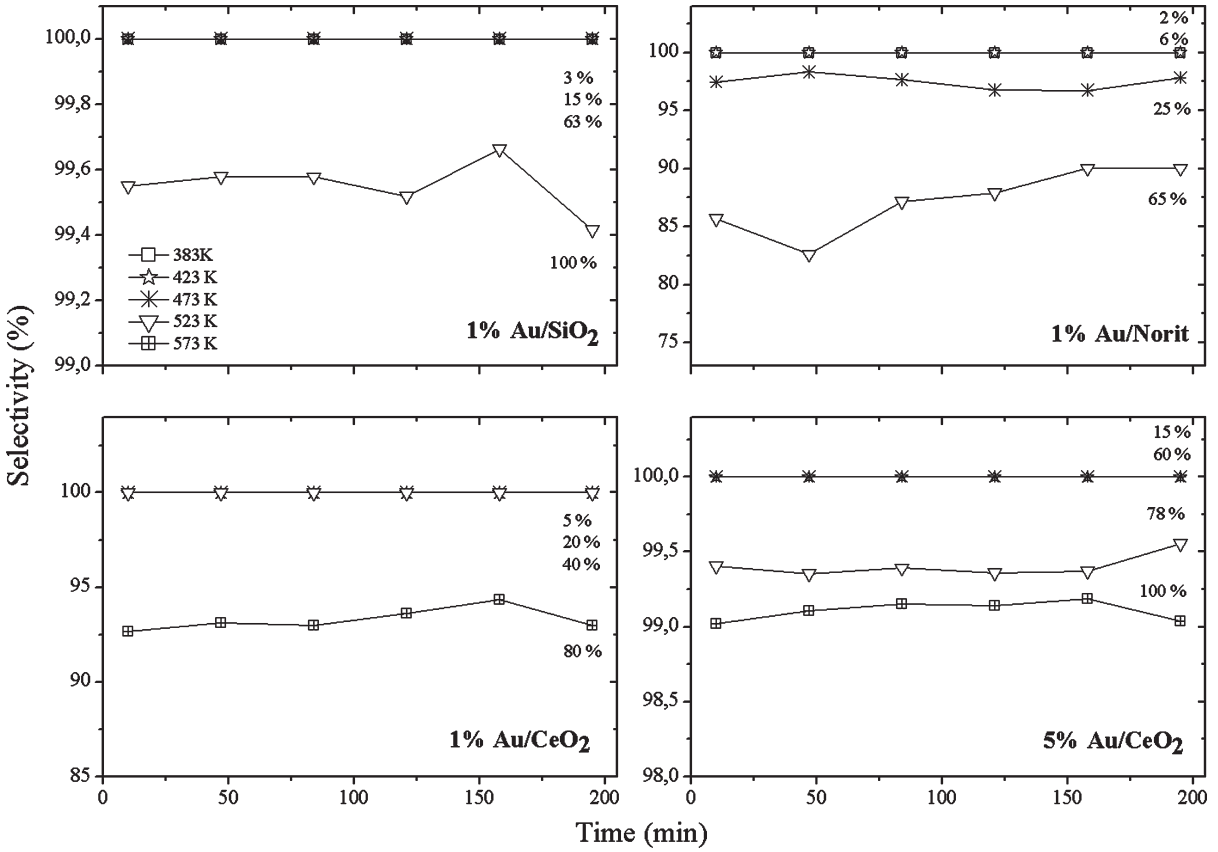

Figure 6. Selectivity of H_2 formation in the reforming of HCOOH (HCOOH/H_2O = 1) on various supported Au catalysts in time on stream at different temperatures. Conversion (in percent) of HCOOH is indicated.

formation. The results on various samples are listed in Table 3. The highest yield (99.5%) was obtained for Au/SiO_2 at 523 K.

4. DISCUSSION

4.1. Adsorption of HCOOH. The adsorption of HCOOH on most of the oxide-supported Au catalysts produced intense absorption bands in the IR spectra (Figure 1). The most important spectral features are the bands at 1555−1600 and 1386−1361 cm^{-1}. The first one is attributed to the asymmetric vibration of formate, whereas the second one to the symmetric stretch of formate.[32] These results indicate that formic acid undergoes dissociation on the samples.

As regards to the location of formate, it is important to point out that we recorded very similar spectra for Al_2O_3 and CeO_2 supports free from Au. We obtained a similar picture in the study of the adsorption of formic acid on supported Rh catalysts.[33] This led to the assumption that the formate species are located on the oxidic supports. This idea was strengthened by the calculation of the number of formate groups, which was 5−8 times higher than that of surface Rh atoms. Further evidence for this assumption was provided by the IR results on Rh/SiO_2, where no formate bands were identified following the adsorption of formic acid at 300 K. It was concluded that no formate exists on SiO_2, and this was confirmed in the present study. As formate was detected on a Rh(111) single crystal by high-resolution electron energy loss spectroscopy below 300 K, it was assumed that HCOOH adsorbs dissociatively on Rh, but the formate produced is unstable and decomposes quickly.[33] As a result, CO is formed, attached to the Rh, giving an intense absorption band at 2030 cm^{-1}, due to Rh_x−CO. This description is very probably valid for the interactions of formic acid with other supported Pt metals.

The situation on supported Au is different, however, as intense formate bands were identified on the FTIR spectra of Au/SiO_2 (Figure 1), which suggests that formate species do exist on Au particles. The spectral features of formate on Au/SiO_2 disappeared only above 573 K, indicating the higher stability of formate on Au as compared to Rh. In light of this, it appears correct to suppose that a Au−formate surface complex also exists on other oxidic supports. Its concentration, however, is incomparable with those of the species bonded to the oxides with high surface areas. This conclusion is strengthened by the TPD results (Figure 2). Only small amounts of decomposition products were observed to desorb from the Au/SiO_2 corresponding to the low concentration of formate on Au. In contrast, larger quantities of H_2, CO, and CO_2 were released from Au/CeO_2 and CeO_2 samples, resulting from the decomposition of formate on the oxides.

4.2. Decomposition and Reforming of Formic Acid. As mentioned in the Introduction, the decomposition of formic acid was a popular model reaction in the 1950s and 1960s to probe the roles of the electronic structures of metals,[18,19] oxides,[20,21] and supported metals.[18,19,22,23] The catalysts found to be active were those able to accept electrons from formic acid or its dissociation products.[18−23] The results obtained for supported metals revealed that variation of the Fermi level of electrons in the n-type TiO_2 support influenced the activation energy of formic acid decomposition measured on Ni.[22] This was explained by the occurrence of an electronic interaction between Ni and n-type

Table 3. Some Characteristic Data for Production of H_2 in Steam Reforming of HCOOH over Supported Au Metal

catalyst	temp. (K)	conv. (%)	H_2 sel. (%)	H_2 yield
1% Au/SiO_2	383	3	100	3
	423	15	100	15
	473	63	100	63
	523	100	99.5	99.5
1% Au/Norit	383	2	100	2
	423	7	100	7
	473	25	97	24.2
	523	66	88	58
1% Au/CeO_2	423	6	100	6
	473	18	100	18
	523	43	100	43
	573	75	93	69.7
5% Au/CeO_2	423	16	100	16
	473	60	100	60
	523	78	99.4	77.5
	573	100	99	99

TiO_2.[22,23] From the aspect of the turnover frequencies, Rh/TiO_2 exhibited the highest activity among the supported Rh samples.[33] Later, more emphasis was placed on the formation and stability of formate on catalyst surfaces.[18,19,34−38] The best catalysts were considered to be those metals on which this surface complex was easily formed, but was not highly stable. Plots of the rate of decomposition at a given temperature as a function of the heat of formation of the corresponding formate yielded "volcano-shaped" curves.[35,36] A more reasonable relationship was presented by Barteau,[37,38] who found a linear correlation between the decomposition temperatures of formates on metals and the heats of formation of the corresponding metal oxides. Au was grouped among the less active metals. This is in harmony with the low affinity of Au for H_2 atoms, which should appear in the dissociation of formic acid, and the cleavage of the C−H bond in the formate.

This correlation, however, was based on results obtained on metal single-crystal surfaces. It has emerged in the past two decades that nanosized Au exhibits surprisingly high catalytic effects in many reactions, including the generation of H_2 in the decomposition of alcohols and dimethyl ether.[10−15] This is the case in the decomposition of formic acid. The catalytic performance of supported Au nanoparticles is comparable with that of supported Rh.[33] On the most active catalyst, Au/SiO_2, the reaction started even at or above 373 K, and complete conversion was attained at 523 K (Figure 3A). In the further interpretation of the results, it should also be taken into account that two reaction pathways can be distinguished in the decomposition of formic acid

$$HCOOH = H_2 + CO_2: \Delta G = -48.4\ \text{kJ mol}^{-1} \quad (1)$$

and

$$HCOOH = H_2O + CO: \Delta G = -28.5\ \text{kJ mol}^{-1} \quad (2)$$

As shown in Figure 3B, the direction of the decomposition depended sensitively on the nature of the supports. Au/SiO_2, Au/Norit, and Au/CeO_2 catalyze almost exclusively the dehydrogenation reaction, particularly at lower temperature. At higher temperatures and conversions, however, the selectivity for H_2 decayed somewhat to extents depending on the catalyst. On other supported Au catalysts, the dehydration reaction (eq 4) was the main process. It is important to point out that no or only very minor changes occurred in the activities and selectivities even after several hours. The possible reason for the absence of deactivation is that CO does not dissociate on the Au catalyst yielding surface carbon.

In situ IR studies revealed the transitional formation of formate species during the reaction at 383−523 K, even on Au/SiO_2, when the formate species are bonded exclusively to the Au particles (Figure 4). This suggests that, similarly as found in some previous studies,[24−28] the decomposition of formic acid proceeds through the formation and decomposition of formate species. We propose the occurrence of the following elementary steps for the decomposition of HCOOH

$$HCOOH_{(g)} = HCOOH_{(a)} \quad (3)$$

$$HCOOH_{(a)} = H_{(a)} + HCOO_{(a)} \quad (4)$$

$$HCOO_{(a)} = CO_{2(a)} + H_{(a)} \quad (5)$$

$$CO_{2(a)} = CO_{2(g)} \quad (6)$$

$$2H_{(a)} = H_{2(g)} \quad (7)$$

The slow step is very probably the rupture of the C−H bond in the adsorbed formate.

From the comparison of TOF values for supported Au samples (Table 2), the highest specific activities in the dehydrogenation reaction were calculated for Au deposited on supports (SiO_2 and Norit) inert toward HCOOH. It appears that the size of Au nanoparticles does not play a determining role. When we can count with the adsorption and reaction of HCOOH on oxidic supports the rate of the dehydrogenation reaction and the selectivity for H_2 formation decreased. An exception is the Au/CeO_2 catalyst, which also exhibited a high catalytic activity in the dehydrogenation of ethanol, which was attributed to the high reactivity of the interface between Au and the partially reduced CeO_2.[14]

An interesting feature of the decomposition of formic acid on these Au catalysts is that the addition of CO to the HCOOH exerted no or only very little influence on the rate and direction of the decomposition. This is in contrast with the results obtained for Rh catalysts, when the decomposition was almost completely suppressed by the presence of CO.[33] FTIR spectroscopy revealed that CO formed in the decomposition is bonded strongly to the Rh and thereby reduces the number of free Rh sites available for the dissociative adsorption of HCOOH. As CO adsorbs weakly on Au particles at and above 300 K, it is not surprising that no deactivation was observed even for Au/Al_2O_3, although a considerable amount of CO was produced in the decomposition on these catalysts.

As the primary aim of this work was to produce CO-free H_2, a great effort was made to enhance the selectivity and the yield of H_2 production. Addition of water to the HCOOH removed the small amount of CO formed on Au/SiO_2 at 473 K, on Au/Norit at 383−423 K, and on Au/CeO_2 at 383−523 K. This is very likely a consequence of the occurrence of the water gas shift reaction:

$$CO + H_2O = CO_2 + H_2 \quad (8)$$

In the other cases, the selectivity could also be enhanced to some extent in the presence of water, but 100% selectivity was not achieved.

Finally, we may compare the results with those obtained in previous papers.[26,27] Although the experimental conditions are different, we can conclude that the catalytic performance of the most active Au/SiO_2 in the decomposition is better than that of the samples used in these studies.[26,27] If we compare the catalytic behavior of Au/Al_2O_3, which was examined before,[27] we can state that our sample is less active and selective for the production of H_2. This can be primarily attributed to the different forms and pretreatments of the supports. With regards to the carbon-supported Au and Pt metals,[28] it appears that the selectivity and the yield for the formation of H_2 in the reforming of HCOOH are higher on Pt metals.

5. CONCLUSIONS

(i) FTIR spectroscopic measurements on Au/SiO_2 demonstrated the dissociative adsorption of formic acid at 300 K and the presence of formate bonded to Au. The formate species formed were detected up to 573 K. In situ IR studies revealed that formate exists on the catalyst surface even during the catalytic reaction at 383−523 K.

(ii) Au metal deposited on various supports was found to be an effective catalyst of the vapor-phase decomposition of formic acid at 373−573 K.

(iii) The reaction pathways of the decomposition were influenced by the nature of the support. High selectivities, 90−100%, were obtained on the catalysts Au/SiO_2, Au/Norit, and Au/CeO_2.

(iv) The addition of water to the formic acid enhanced the yield and selectivity of H_2 production.

AUTHOR INFORMATION

Corresponding Author

*Fax: +36-62-544-106. E-mail: fsolym@chem.u-szeged.hu.

ACKNOWLEDGMENT

This work was supported by the grant OTKA under contract number K 81517.

REFERENCES

(1) Haryanto, A.; Fernando, S.; Murali, N.; Adhikari, S. *Energy Fuels* **2005**, *19*, 2098–2106.

(2) Sandstede, G.; Veziroglu, T. N.; Derive, C.; Pottier, J., Eds.; *Proceedings of the Ninth World Hydrogen Energy Conference*, Paris, France, 1972; pp 1745−1752.

(3) Faungnawakij, K.; Shimoda, N.; Fukunaga, T.; Kikuchi, R.; Eguchi, K. *Appl. Catal., B* **2009**, *92*, 341–350 and references therein.

(4) Solymosi, F.; Kutsán, Gy.; Erdöhelyi, A. *Catal. Lett.* **1991**, *11*, 149–156.

(5) Belgued, M.; Amariglio, H.; Pareja, P.; Amariglio, A.; Sain-Just, J. *Catal. Today* **1992**, *13*, 437–445.

(6) Koerts, T.; Deelen, M. J. A. G.; van Santen, R. A. *J. Catal.* **1992**, *138*, 101–114.

(7) Barthos, R.; Széchenyi, A.; Koós, Á.; Solymosi, F. *Appl. Catal., A* **2007**, *327*, 95–105.

(8) Koós, Á.; Barthos, R.; Solymosi, F. *J. Phys. Chem. C* **2008**, *112*, 2607–2612.

(9) Solymosi, F.; Barthos, R.; Kecskeméti, A. *Appl. Catal., A* **2008**, *350*, 30–37.

(10) Haruta, M.; Kobayashi, T.; Sano, H.; Yamada, N. *Chem. Lett.* **1987**, *16*, 405–408.

(11) Hashmi, A. S. K.; Hutchings, G. J. *Angew. Chem., Int. Ed.* **2006**, *45*, 7896–7936.

(12) Bond, G. C.; Louis, C.; Thompson, D. T. *Catalysis by Gold*; Imperial College Press: London, 2006.

(13) Gazsi, A.; Bánsági, T.; Solymosi, F. *Catal. Lett.* **2009**, *131*, 33–41.

(14) Gazsi, A.; Koós, Á.; Bánsági, T.; Solymosi, F. *Catal. Today* **2011**, *160*, 70–78.

(15) Gazsi, A.; Ugrai, I.; Solymosi, F. *Appl. Catal., A* **2011**, *391*, 360–366.

(16) Choi, J. H.; Jeong, K. J.; Dong, Y.; Han, J.; Lim, T. H.; Lee, J. S.; Sung, Y. E. *J. Power Sources* **2006**, *163*, 71–75 and references therein.

(17) Fellay, C; Dyson, P. J.; Laurenczy, G. *Angew. Chem., Int. Ed.* **2008**, *47*, 3966–3968.

(18) Bond, G. C. *Catalysis by Metals*; Academic: London, 1962.

(19) Mars, P.; Scholten, J. J. F.; Zwietering, P. *Adv. Catal.* **1963**, *14*, 35–113.

(20) Szabó, Z. G.; Solymosi, F. *Acta Chim. Hung.* **1960**, *25*, 145.

(21) Trillo, J. M.; Munuera, G.; Criado, J. M. *Catal. Rev.* **1972**, *7*, 51–86.

(22) Szabó, Z. G.; Solymosi, F. *Actes Congr. Int. Catal., 2nd* **1961**, 1627–1648.

(23) Solymosi, F. *Catal. Rev.* **1968**, *1*, 233–255.

(24) Koós, Á.; Solymosi, F. *Catal. Lett.* **2010**, *138*, 23–27.

(25) Zhou, X.; Huang, Y.; Xing, W.; Liu, C.; Liao, J.; Lu, T. *Chem. Commun.* **2008**, 3540–3542.

(26) Ojeda, M.; Iglesia, E. *Angew. Chem., Int. Ed.* **2009**, *48*, 4800–4803.

(27) Bulushev, D. A.; Beloshapkin, S.; Ross, J. R. H. *Catal. Today* **2010**, *154*, 7–12.

(28) Solymosi, F.; Koós, Á.; Liliom, N.; Ugrai, I. *J. Catal.* **2011**, *279*, 213–219.

(29) Boddien, A.; Gärtner, F.; Jackstell, R.; Junge, H.; Spannenberg, A.; Baumann, W.; Ludwig, R.; Beller, M. *Angew. Chem., Int. Ed.* **2010**, *49*, 8993–8996.

(30) Fellay, C.; Dyson, P. J.; Laurenczy, G. *Angew. Chem., Int. Ed.* **2008**, *47*, 3966–3968.

(31) Enthaler, S.; von Langermann, J.; Schmidt, T. *Energy Environ. Sci.* **2010**, *3*, 1207–1217 and references therein.

(32) Kecskés, T.; Raskó, J.; Kiss, J. *Appl. Catal., A* **2004**, *268*, 9–16 and references therein.

(33) Solymosi, F.; Erdőhelyi, A. *J. Catal.* **1985**, *91*, 327–337.

(34) Eischens, R. E.; Pliskin, W. A. *Actes Congr. Int. Catal., 2nd* **1961**, 789.

(35) Sachtler, W. M. H.; Fahrenfort, J. *Actes Congr. Int.Catal., 2nd* **1961**, 831.

(36) Madix, R. J. *Adv. Catal.* **1980**, *29*, 1–53.

(37) Barteau, M. A. *Catal. Lett.* **1991**, *8*, 175–183.

(38) Mavrikakis, M.; Barteau, M. A. *J. Mol. Catal. A: Chem.* **1998**, *131*, 135–147.